



Contents lists available at ScienceDirect

Journal of Traditional and Complementary Medicine

journal homepage: [www.elsevier.com/locate/jtcm](http://www.elsevier.com/locate/jtcm)

# Zhilong Huoxue Tongyu capsule protects against atherosclerosis by suppressing EndMT via modulating Hippo/YAP signaling pathway

Yanan Zhou<sup>a,b,1</sup>, Hong Wang<sup>a,b,1</sup>, Tao Bi<sup>a,b</sup>, Pan Liang<sup>a,b</sup>, Xinyue Liu<sup>a,b</sup>, Hongping Shen<sup>a,b</sup>, Qin Sun<sup>a,b</sup>, Gang Luo<sup>b,c</sup>, Ping Liu<sup>b,c</sup>, Sijin Yang<sup>a,b,c,\*\*</sup>, Wei Ren<sup>a,b,\*</sup><sup>a</sup> National Traditional Chinese Medicine Clinical Research Base and Drug Research Center of Integrated Traditional Chinese and Western Medicine, The Affiliated Traditional Chinese Medicine Hospital, Southwest Medical University, Luzhou, Sichuan, China<sup>b</sup> Institute of Integrated Chinese and Western Medicine, Southwest Medical University, Luzhou, Sichuan, China<sup>c</sup> Department of Cardiovascular Medicine, The Affiliated Traditional Chinese Medicine Hospital, Southwest Medical University, Luzhou, Sichuan, China

## ARTICLE INFO

### Keywords:

Atherosclerosis  
Zhilong huoxue tongyu  
Capsule  
Traditional Chinese  
Medicine  
Endothelial-to-mesenchymal  
Transition  
Hippo/YAP signaling  
Pathway

## ABSTRACT

**Background and aim:** Zhilong Huoxue Tongyu Capsule (ZL capsule) has been demonstrated to be an effective and widely-used traditional Chinese medicine (TCM) formula for the treatment of various diseases, especially for atherosclerosis (AS) related cardiovascular and cerebrovascular diseases. Reversal of endothelial-mesenchymal transition (EndMT) plays a crucial role in the cure of AS. But the curative impact of ZL capsule on EndMT remains obscure during the development of AS. The purpose of this study is to explore the effect of ZL capsule on AS and to study the regulation mechanism on EndMT in AS by ZL capsule *in vivo* and *in vitro*.

**Experimental procedure:** An *in vivo* model of AS was induced in ApoE<sup>-/-</sup> mice by administrating them with an 8-week period of high-fat diet (HFD). After oral gavage of different doses of ZL capsule and Atorvastatin calcium tablets (ATO) for 4 weeks, the lipid levels, plaque area, lipid deposition, and EndMT were evaluated using standard assays. In order to simulate EndMT *in vitro*, human umbilical vein endothelial cells (HUVECs) were subjected to oxidized low-density lipoprotein (ox-LDL). Western blotting (WB) and immunofluorescence techniques were used to evaluate the intervention effect of ZL capsule on EndMT and Hippo/YAP pathways.

**Results and conclusion:** ZL capsule demonstrated therapeutic effects on dyslipidemia and EndMT among atherosclerotic mice. To be specific, ZL capsule diminished the total cholesterol (TC), total triglyceride (TG) and low-density lipoprotein (LDL-C) levels, whereas increased that of high-density lipoproteins (HDL-C). Meanwhile, ZL capsule upregulated the expression of endothelial markers (CD31 and VE-cadherin) and reduced that of mesenchymal markers ( $\alpha$ -SMA and FSP1), indicating that ZL capsule could inhibit EndMT during the development of AS. Furthermore, molecular docking results indicated that active ingredients including formononetin, calycosin, astragaloside III, astragaloside A in ZL capsule have strong affinity with YAP proteins, and ZL capsule can significantly repress the initiation of Hippo/YAP pathway during AS. In conclusion, ZL capsule effectively attenuated AS progression by exerting inhibitory effects on EndMT through modulation of the Hippo/YAP signaling pathway.

## 1. Introduction

Cardiovascular disease (CVD) has an increasing global impact due to rising incidence, poor prognosis, and high mortality.<sup>1</sup> According to

epidemiological evidence, the number of patients with cardiovascular diseases worldwide is increasing year by year, from 271 million in 1990 to 523 million in 2019.<sup>2</sup> Atherosclerosis (AS), a commonly occurring chronic vascular disorder, is the principal stimulus of cardiovascular and

Peer review under responsibility of The Center for Food and Biomolecules, National Taiwan University.

\* Corresponding author. 182# chunhui road, Luzhou, Sichuan, 646000, China.

\*\* Corresponding author. 182# chunhui road, Luzhou, Sichuan, 646000, China.

E-mail addresses: [18703667421@163.com](mailto:18703667421@163.com) (Y. Zhou), [hwang0324@163.com](mailto:hwang0324@163.com) (H. Wang), [bitao456321@163.com](mailto:bitao456321@163.com) (T. Bi), [xnydzyylp@swmu.edu.cn](mailto:xnydzyylp@swmu.edu.cn) (P. Liang), [lxyue1119@163.com](mailto:lxyue1119@163.com) (X. Liu), [15082068899@163.com](mailto:15082068899@163.com) (H. Shen), [496655521@qq.com](mailto:496655521@qq.com) (Q. Sun), [1982luogang@163.com](mailto:1982luogang@163.com) (G. Luo), [helloliuping@swmu.edu.cn](mailto:helloliuping@swmu.edu.cn) (P. Liu), [ysjimm@sina.com](mailto:ysjimm@sina.com) (S. Yang), [renwei1991@swmu.edu.cn](mailto:renwei1991@swmu.edu.cn) (W. Ren).

<sup>1</sup> These authors contributed equally to this work.

<https://doi.org/10.1016/j.jtcm.2024.03.015>

Received 18 October 2023; Received in revised form 17 March 2024; Accepted 26 March 2024

Available online 29 March 2024

2225-4110/© 2024 Center for Food and Biomolecules, National Taiwan University. Production and hosting by Elsevier Taiwan LLC. This is an open access article under the CC BY-NC-ND license (<http://creativecommons.org/licenses/by-nc-nd/4.0/>).

cerebrovascular diseases such as hypertensive disease and coronary artery disease.<sup>3,4</sup> Atherosclerosis (AS) is a common disease and one of the main causes of cardiovascular and cerebrovascular diseases such as hypertension and coronary heart disease,<sup>5</sup> among which endothelial dysfunction has received increasing attention from many researchers.<sup>6</sup> There is growing evidence that endothelial cells (ECs) play a key role in every stage in the development of AS, from atherosclerosis to the formation and expansion of atherosclerotic plaques and necrosis, plaque rupture and clinical manifestations.<sup>7</sup> ECs are important participants in the intravascular immune response, promoting the recruitment of white blood cells during inflammatory responses or infections, and releasing cytokines and chemokines that result in the buildup and penetration of monocytes and other cells associated with inflammation, ultimately leading to endothelial dysfunction and vascular damage.<sup>7,8</sup> Endothelial dysfunction then triggers the atherogenic process by promoting platelet aggregation, lipoprotein oxidation, thrombosis and inflammation.<sup>9</sup>

Endothelial-mesenchymal transition (EndMT) is the pivotal process resulting in endothelial dysfunction, which has been widely acknowledged for its indispensable role in the intricate development of vascular inflammation and atherosclerosis.<sup>10,11</sup> During the EndMT process, ECs lose their property of down-regulating endothelial cell markers, such as CD31 and VE-cadherin,  $\alpha$ -smooth muscle actin ( $\alpha$ -SMA), fibroblast-specific protein 1 (FSP1) and vimentin.<sup>12</sup> The transformed cells resulting from EndMT can migrate towards plaque-prone areas, and these migrated cells can further differentiate into smooth muscle-like cells or fibroblasts contributing to neointima formation or fibrous cap thickening respectively.<sup>13,14</sup> All these pathological alterations intensify the progression of AS. Therefore, it is necessary to identify and validate potential therapies for inhibiting EndMT to effectively treat AS.

The Hippo signaling pathway plays an important role in controlling cell growth and maintaining organ size. When Hippo is activated, Yes-related transcription proteins/coactivators with PDZ-binding motifs (YAP/TAZ) are phosphorylated, retained in the cytoplasm, and then gradually degraded.<sup>15</sup> When Hippo is inactivated, YAP/TAZ is dephosphorylated and translocated to the nucleus. This phenomenon triggers the expression of target genes, controls the functional status of smooth muscle cells and affects vascular remodeling.<sup>16</sup> Therefore, targeted inhibition of Hippo/YAP signaling activation may attenuate inflammatory responses, inhibit vascular remodeling, stabilize arterial plaques, and slow down AS progression by inhibiting YAP/TAZ activation.

Zhilong Huoxue Tongyu capsule (Patent No.: 200810147774.1) is a patented traditional Chinese medicine preparation composed of *astragalus*, *leeches*, *earthworms*, *cinnamon*, and *wild ginseng*.<sup>17,18</sup> For more than 20 years, ZL capsule has been used clinically as an effective herbal medicine to treat AS related cardiovascular diseases.<sup>19,20</sup> Recently, our group has also reported that ZL capsule could improve AS through inhibiting the interplay between miR-30b-5p and NLRP3.<sup>21</sup> Both clinical trials and animal experiments demonstrate that ZL capsule has the ability to effectively reduce levels of total cholesterol (TC), total triglyceride (TG), and low-density lipoprotein cholesterol (LDL-C) in the bloodstream, whereas simultaneously enhancing high-density lipoprotein (HDL-C).<sup>17</sup> However, the regulatory effect of ZL capsule on EndMT in the process of AS has not been evaluated, and the intervention mechanism on EndMT has not been explored. Herein, in this study, the impact of ZL capsule on EndMT during AS was further clarified *in vitro* and *in vivo*. Further, the pharmacological mechanism of ZL capsule on EndMT was explored, which may shed new lights on the application of ZL capsule as a potential therapeutic agent targeting AS.

## 2. Materials and methods

### 2.1. Chemicals and reagents

ZL capsule was purchased from the Affiliated Traditional Chinese Medicine Hospital of Southwest Medical University (Luzhou, Sichuan, China, Batch No. 20210619). Atorvastatin was purchased from the

MedChemExpress (CAT: HY-B0589).

We purchased the following antibodies:  $\alpha$ -Actin (Santa Cruz, sc-32251), CD31 (BD Biosciences, 553370), FSP1 (Proteintech, 20886-1-AP), CD68 (Proteintech, 28058-1-AP), YAP (Proteintech, 13584-1-AP), WWTR1 (Proteintech, 66500-1-Ig), and VE-cadherin (Proteintech, 66804-1-Ig) from Proteintech.

### 2.2. Animals and treatment

The male ApoE<sup>-/-</sup> mice (weighing 20–22 g and aged 6–8 weeks) were obtained from GemPharmatech Co.Ltd and acclimatized for one week. The mice were adapted for 22  $\pm$  0.5 °C under a 12 h light/dark cycle with unrestricted access to a conventional diet and water for drinking. The protocols for animal care and handling were approved by the Animal Research Committee of Southwest Medical University. The 30 mice were separated into two groups: the normal control group, which received a regular diet (ND), and four other groups (each consisting of 6 mice) that were given a high fat diet (HFD) for a duration of 8 weeks in order to induce AS. Further, the HFD-fed animals were randomly assigned to different groups: untreated model group (HFD), low-dose ZL-LD group (0.35 g/kg), medium dose ZL-MD group (0.7 g/kg), high dose ZL-HD group (1.4 g/kg), and positive control group treated with 5 mg/kg simvastatin. The prepared ZL capsule extract was administered to AS mice orally once daily at 2 mL/100 g body weight for 4 weeks.

### 2.3. Serum lipid content detection

At the end of the experiment, blood samples were obtained from the orbital vein while the subject was under anesthesia. The samples were collected and stored at room temperature for 1–2 h, and sera were isolated by centrifuging at 3000 rpm for 15 min at 4 °C, and preserved at –80 °C. Plasma TC, TG, LDL and HDL were determined with commercially available kits (Jiancheng Bioengineering Institute, Nanjing, China).

### 2.4. Hematoxylin and eosin (H&E) staining

After the experiment, the aortic sinus tissue was excised and stored in 4% paraformaldehyde for 72 h. Further, the samples were embedded in paraffin and sectioned into 4  $\mu$ m thick. Paraffin sections were deparaffinized in xylene and then rehydrated in ethanol at concentrations of 100%, 95%, 90%, and 85%. Hematoxylin staining was performed for 10 min, and sections were graded in acid alcohol for 5 s. The membrane was then washed with 75% alcohol and stained with eosin for 2 min. Dehydrated in an ethanol gradient and cleared in xylene for 5 min, the sections were then covered with neutral gel and examined under a microscope.

### 2.5. Oil Red O staining

Aortic samples were fixed in 4% paraformaldehyde for 3–6 h and washed three times for 10 min each in PBS. After removing adjacent connective tissue and fat, staining was performed using Oil Red O working solution (Sigma, Deisenhoggfen, Germany) for 30 min at 37 °C. The cells were then washed three times with PBS for 10 min each time. The samples were then rinsed with 75% ethanol for 2 min. Subsequently, PBS was used for washing the samples before imaging.

### 2.6. Immunofluorescent staining of aortic samples

For immunofluorescence staining, 4  $\mu$ m thick cryosections were prepared from aortic samples and immersed in a solution containing 4% paraformaldehyde. Sections were first fixed with 5% goat serum, treated with primary antibodies and incubated overnight at 4 °C. After washing 3 times with PBS (including a 10-min wash), the slides were exposed to

secondary antibodies for 1 h. Finally, sections were counterstained with DAPI (Beyotime, C1002) for 10 min, rinsed with PBS, stored in 20% glycerol, and photographed.

### 2.7. Cytotoxicity assay

Cell viability assay was used to evaluate the effect of ZL capsule on HUVECs. HUVECs were cultured in a 96-well plate at of  $5 \times 10^3$  cells/well. The cells were then cultured for 48 h with various chemical doses overnight at 37 °C in an incubator with 5% CO<sub>2</sub>. Afterward, 100 μL of the detection reagent Cell Titer-Lumi Plus (Beyotime, CAT:C0068 M) was added to each well, and the wells were vibrated for 5 min to completely lyse the cells. Each well's luminescence (RLU) was measured using a luminometer with a multipurpose microplate reader. The values of the test wells' absorbance were recorded as RLU treatment while the values of the negative controls' absorbance were recorded as RLU controls, and the values of the blank were recorded as RLU blank for each assay. Inhibition rate (%) =  $(RLU_{\text{control}} - RLU_{\text{blank}} - RLU_{\text{treated}}) / (RLU_{\text{control}} - RLU_{\text{blank}}) * 100$ , IC<sub>50</sub> values were calculated using GraphPad Prim 8.0 software.

### 2.8. Western blotting

The protein extraction was performed using a cold RIPA lysis buffer (Beyotime, CAT: P0013B), and the quantification of protein was carried out using the bicinchoninic acid (BCA) assay. The protein samples underwent separation using SDS-PAGE and were subsequently transferred onto PVDF membranes (Merck Millipore, CAT: IPVH00010). After incubating in 5% bovine serum albumin (BSA) at 37 °C for 2 h, primary antibodies such as α-SMA (1:1000), FSP1 (1:1000), CD31 (1:1000), VE-cadherin (1:1000), and GAPDH (1:5000) were added overnight at 4 °C. After washing, secondary antibodies labeled with HRP were incubated at a temperature of 37 °C for 1 h. The bands were visualized using ECL blotting technique (Beyotime, CAT: P0018S).

### 2.9. Statistical analysis

Data analysis was performed using Paradigm 9 in GraphPad. In this study, comparative analysis was performed using two-tailed *t*-test to examine the differences between two different groups. *P* value of less than 0.05 was considered statistically significant.

## 3. Results

### 3.1. ZL capsule improved atherosclerotic lesions and lipid deposition in ApoE<sup>-/-</sup> mice

To explore the efficacy of ZL capsule on atherosclerotic lesions, we established an AS model using ApoE<sup>-/-</sup> mice fed with HFD, and administered the animals with varying amounts of ZL capsule or ATO. In light of the association between atherosclerotic plaque development and heightened cholesterol levels in the bloodstream, we conducted an evaluation of blood lipid profiles in mice subsequent to a 4-week drug administration. As shown in Fig. 1A, after being subjected to HFD, ApoE<sup>-/-</sup> mice displayed notably elevated serum levels of LDL-C, TC, and TG, while concurrently experiencing a notable decrease in HDL-C. And after administration of ZL capsule, the levels of HDL-C, LDL-C, TC, and TG were improved (Fig. 1A). To further assess the efficacy of ZL capsule in alleviating symptoms associated with AS, we conducted histological examination using HE staining and Oil Red O staining on the aortic root. The findings suggest that there is a substantial decrease in lipid accumulation and atherosclerotic plaque lesion areas in mice treated with a high dose of ZL capsule or ATO compared with the untreated HFD-fed animals (Fig. 1B). CD68<sup>+</sup> macrophages can serve as valuable indicators for evaluating plaque stability in the progression of AS.<sup>22</sup> Therefore, we conducted immunofluorescence staining experiments

targeting CD68 in the aortic roots of mice. The results clearly showed that the expression of CD68 in plaques was reduced in mice treated with high doses of ZL capsule or ATO compared with the untreated mice fed with HFD (Fig. 1C). These findings provided further validation that ZL capsule can impair dyslipidemia metabolism and attenuate the symptoms of AS.

### 3.2. ZL capsule inhibited the development of EndMT during atherosclerotic *in vivo*

To estimate the potential impact of ZL capsule on EndMT, we performed double-staining experiments for CD31/α-SMA and CD31/FSP1 in mouse aortic roots. The experimental results showed that stronger signal of α-SMA/FSP1 was observed in the CD31 expression region compared with the control group (Fig. 2A and B). After administration of ZL capsule or ATO, the signal of α-SMA/FSP1 in the CD31 expression region was significantly reduced (Fig. 2A and B). The findings indicated that ZL capsule could ameliorate AS by inhibiting EndMT.

### 3.3. ZL capsule inhibited the development of ox-LDL-induced EndMT in HUVECs

In this study, we employed the CCK8 method to appraise the impact of ZL capsule on HUVECs, and the outcomes indicated that ZL capsule exhibited minimal cytotoxicity (Fig. 3A). Further, additional validation was conducted to confirm the effect of ZL capsule on inhibiting EndMT in HUVEC cell lines. As ox-LDL has the ability to disrupt the integrity of the ECs barrier within blood vessels and initiate EndMT, it is commonly used as an *in vitro* stimulus to simulate the process of atherosclerosis-induced EndMT. We observed consistent alterations in the levels of CD31 and α-SMA in HUVECs exposed to ox-LDL for a duration of 48 h, mirroring those observed in an *in vivo* model. In addition, compared with the control group, ox-LDL exhibited a downregulating effect on the expression of CD31 and VE-cadherin genes, while concurrently upregulating the gene expression of FSP1 and α-SMA (Fig. 3B). However, ZL capsule effectively counteracted the alterations in the aforementioned factors that were triggered by oxidized low-density lipoprotein (Fig. 3B). EndMT is distinguished by the disruption of cell-cell adhesion and cellular orientation, leading to the acquisition of a spindle-shaped morphology and the development of migratory and invasive characteristics, accompanied by an enhanced production of extracellular matrix. As illustrated in Fig. 3C, the exposure to ox-LDL triggers a notable alteration in the morphology of HUVECs, transitioning them from a cobblestone-like appearance to a spindle-shaped configuration, but ZL capsule effectively blocked OX-LDL-induced changes in HUVEC morphology. At the same time, the results of the immunofluorescence staining demonstrated a significant reduction in the overexpression of α-SMA induced by ox-LDL following the administration of ZL capsule (Fig. 3D). Accordingly, the results indicate that ZL capsule has the ability to impede EndMT *in vitro*.

### 3.4. YAP is a potential target for ZL capsule to inhibit EndMT and reduce AS

Recent research has revealed remarkable therapeutic potential of YAP protein-targeting drugs in combating AS. In our previous study, we characterized the active ingredients of ZL capsule and identified a total of 12 components including astragaloside A, astragaloside I, astragaloside II, astragaloside III, chlorogenic acid, L-epicatechin, calycosin, wogonin, formononetin and calycosin-7-glucoside.<sup>23</sup> To further substantiate the intervention potential of ZL capsule on Hippo/YAP signaling, we performed molecular docking simulations between 12 compounds derived from ZL capsule and YAP protein (Fig. 4A). Generally, the lower the binding energy of ligand-receptor docking indicates the more robust binding of the molecule, with more robust binding at binding energies ≤ -5.0 kcal·mol<sup>-1</sup> and very robust binding at binding

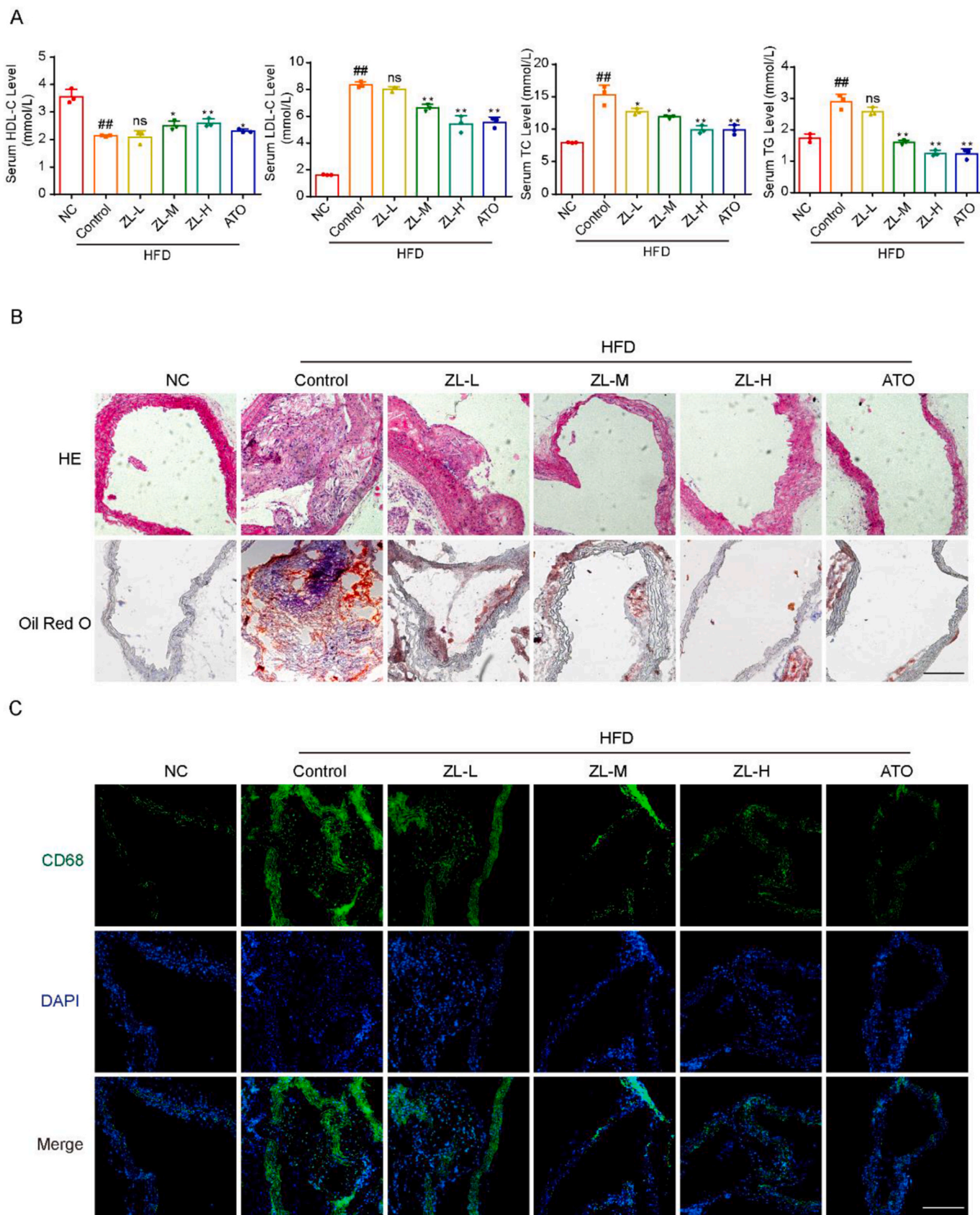


**Fig. 1.** ZL capsule reduced AS lesions and lipid buildup in ApoE<sup>-/-</sup> mice. (A) Serum levels of HDL-C, LDL-C, TC and TG in the indicated groups (n = 4). (B) Representative images of HE-stained/Oil red O-aortic root sections that have been stained to reveal the presence of atherosclerotic plaques (n = 4). Scale bar = 100 μm. (C) Representative immunofluorescence images are presented to demonstrate the in-situ expression of CD68 in sections of the aorta root (n = 4). Scale bar = 100 μm. All results are presented as the average ± S.D. The statistical significance was observed at  $p < 0.05^*$  and  $p < 0.01^{**}$  levels.

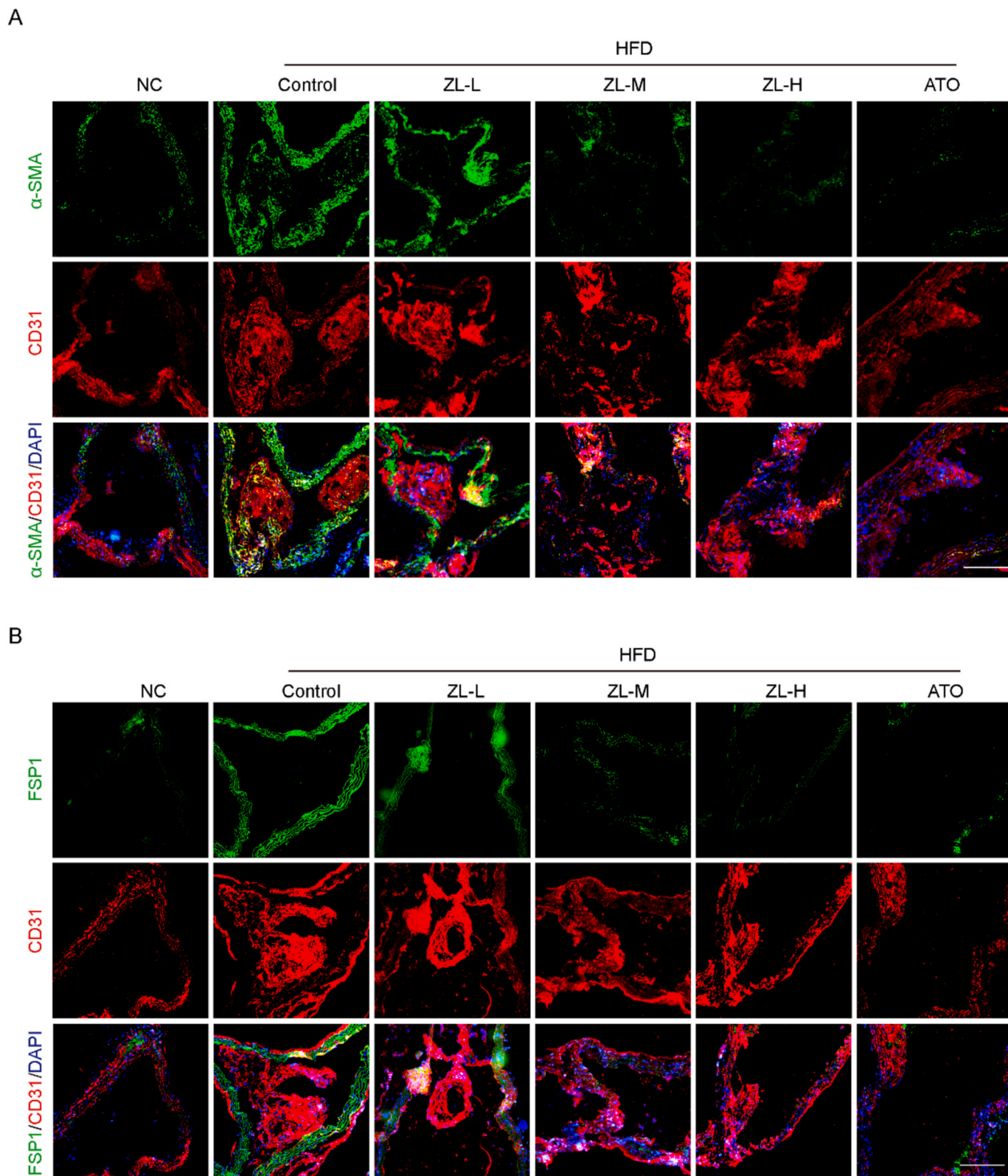


**Fig. 2.** ZL capsule inhibited the development of EndMT during AS *in vivo*. **(A)** Immunofluorescent staining against  $\alpha$ -SMA (green) and CD31 (red), counterstaining with DAPI (blue: nuclei) from the indicated experimental groups (n = 4) after HFD-induced atherosclerosis. Scale bar: 100  $\mu$ m. **(B)** Immunofluorescent staining against FSP1 (green) and CD31 (red), counterstaining with DAPI (blue: nuclei) from the indicated experimental groups (n = 4) after HFD-induced atherosclerosis. Scale bar: 100  $\mu$ m.

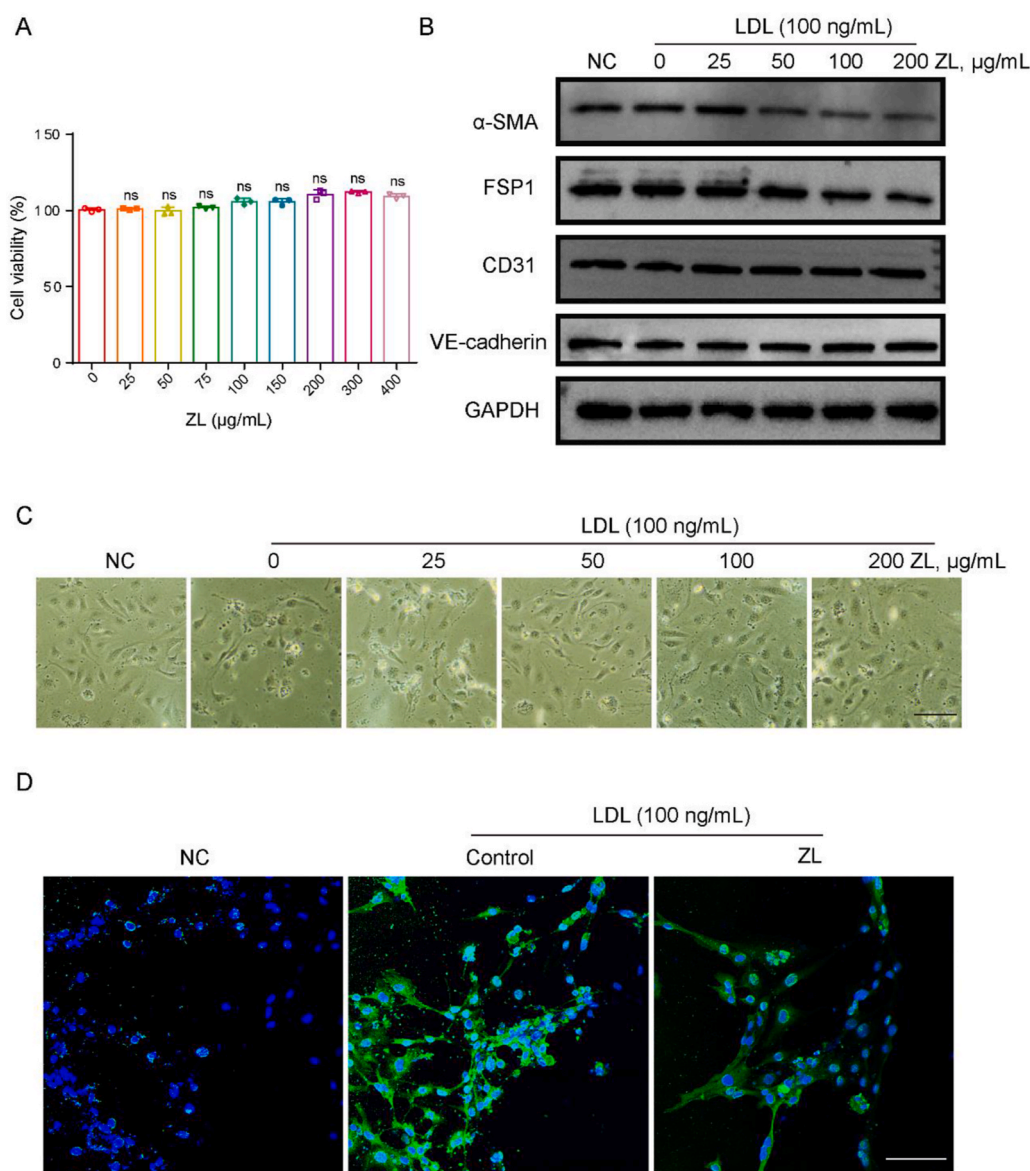


**Fig. 3.** ZL capsule inhibited the development of ox-LDL-induced EndMT in HUVECs. (A) The cell viability was determined after HUVECs were incubated with various concentrations of ZL capsule for 48 h. (B) The expression of EndMT-related proteins including  $\alpha$ -SMA, FSP1 and CD31 after ZL capsule treatment, were compared among ox-LDL and ZL capsule groups in HUVECs. (C) Morphological change in HUVECs was observed by microscopy. Scale bar = 100  $\mu$ m. (D) Immunofluorescent staining against  $\alpha$ -SMA (green) and counterstaining with DAPI (blue: nuclei) in HUVECs. Scale bar: 100  $\mu$ m.

energies  $\leq -7.0$  kcal-mol<sup>-1</sup>. The experimental results indicate a robust binding affinity between the YAP protein and the aforementioned 12 compounds (Fig. 4B). In order to further clarify the binding potential of active ingredients in ZL capsules to YAP protein, we further analyzed the binding sites and binding forces of formononetin, calycosin, astragaloside III, astragaloside A and YAP protein with strong binding forces. It was found that formononetin, calycosin, astragaloside III, astragaloside A and YAP proteins have multiple binding sites (Fig. 4C). They interfere with YAP protein activity by forming  $\pi$ - $\pi$  coupling with YAP protein amino acid residues and forming van der Waals forces. Through the analysis of the experimental results of molecular dynamics simulation, we found that components including formononetin, calycosin, astragaloside III, astragaloside A in ZL capsule had strong affinity with YAP protein.

### 3.5. ZL capsule inhibits the Hippo/YAP signal pathway during AS

WB results revealed that stimulation with ox-LDL induced a

significant upregulation of YAP and its downstream effectors TAZ in HUVECs. However, treatment with ZL capsule effectively reversed the ox-LDL-induced upregulation of these factors (Fig. 5A). To further substantiate the efficacy of ZL capsule in modulating Hippo/YAP signaling, we conducted an *in vivo* assessment of the intervention effect exerted by ZL capsule on Hippo/YAP signaling. The immunofluorescence results demonstrated a significant inhibition in the expression of YAP and TAZ following treatment with ZL capsule (Fig. 5B). The results mentioned above suggest that ZL capsule possessed a strong intervention effect on Hippo/YAP signaling pathway in the process of atherosclerosis.

## 4. Discussion

EndMT plays an important role in the occurrence and development of cardiovascular and cerebrovascular diseases.<sup>24</sup> Vascular endothelial dysfunction disrupts endothelial integrity and barrier function and promotes lipid deposition. EC dysfunction is one of the lesions that can be detected in the early stages of atherosclerosis.<sup>25,26</sup> Currently, the

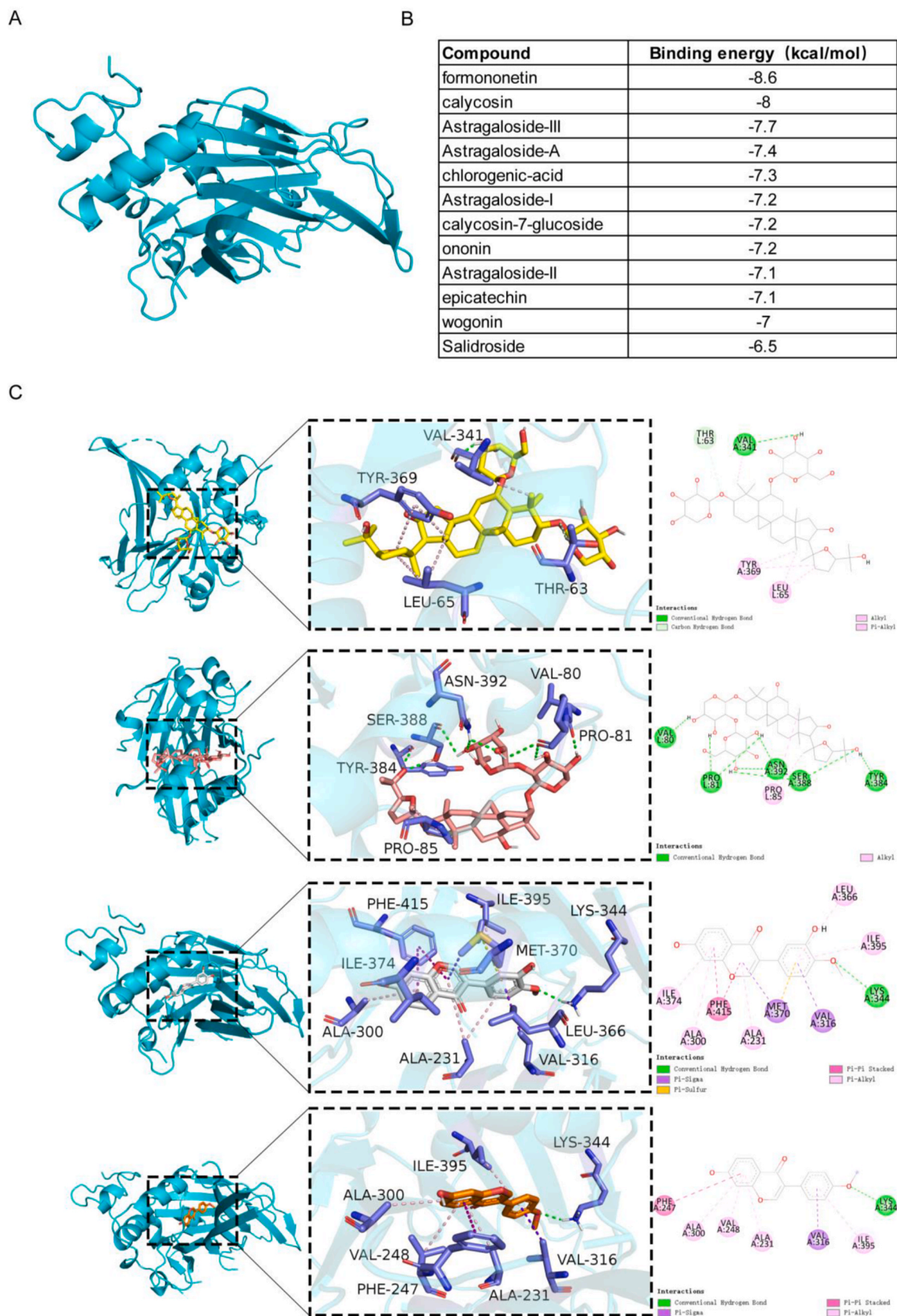


**Fig. 4.** YAP is a potential target for ZL capsule to hinder EndMT and reduce AS. (A) The spatial structure of YAP. (B) The binding energy between YAP and astragaloside A, astragaloside I, astragaloside II, astragaloside III, chlorogenic acid, L-epicatechin, calycosin, wogonin, formononetin and calycosin-7-glucoside. (C) The docking diagram and the 3D diagram of the interaction between formononetin, calycosin, astragaloside III, astragaloside A and BRD4.

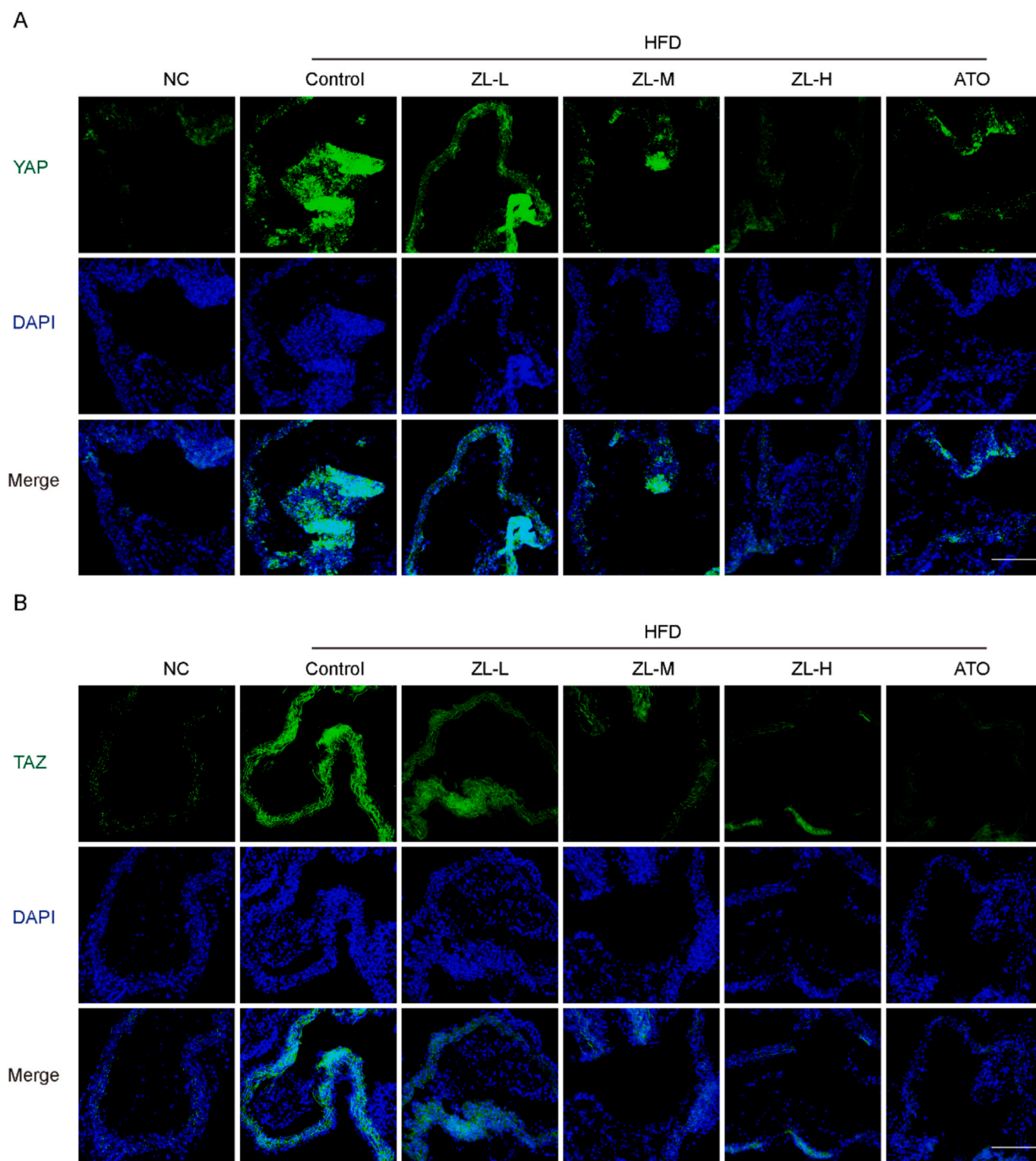


**Fig. 5.** ZL capsule inhibits the Hippo/YAP signal pathway during AS. (A) Immunofluorescent staining against YAP (green), counterstaining with DAPI (blue: nuclei) from the indicated experimental groups (n = 4) after HFD-induced atherosclerosis. Scale bar: 100 μm. (B) Immunofluorescent staining against TAZ (green) and CD31 (red), counterstaining with DAPI (blue: nuclei) from the indicated experimental groups (n = 4) after HFD-induced atherosclerosis. Scale bar: 100 μm.

involvement of EndMT is believed to be crucial in causing damage to ECs.<sup>27</sup> The purpose of this study was to evaluate the therapeutic effect of ZL capsules on EC dysfunction and its underlying mechanisms. It was observed that the administration of ZL capsule mitigated EndMT induced by HFD and also attenuated EndMT stimulated by ox-LDL in HUVECs.

In recent years, the application of traditional Chinese medicine in the prevention and treatment of AS has been increasing.<sup>28</sup> Extensive basic and clinical research provides sufficient evidence for the beneficial effects of ZL capsules on AS<sup>17</sup>. Our previous study showed that ZL capsule has a dose-dependent protective effect on AS. In the present study, we evaluated the therapeutic effect of ZL capsule on AS by detecting the



contents of TC, TG, LDL-C and HDL-C. The results showed that ZL capsule significantly reduced TC, TG and LDL-C of HFD-induced mice, and obviously increased HDL-C. In addition, we found that ZL capsule can significantly improve the vascular structure, reduce the deposition of lipids, and inhibit the aggregation of macrophages in the process of AS. As a result, the utilization of ZL capsule can effectively improve lipid metabolism disorders and alleviate AS symptoms during the development of atherosclerosis. ECs undergoing EndMT transformation can aggravate AS symptoms by stimulating inflammation responses, inducing lipoprotein oxidation, platelet aggregation, and thrombosis.<sup>29</sup> We also found that ZL capsule can considerably reduce the proliferation of ECs and the acquisition of mesenchymal features during AS *in vivo*. Further, we tested the intervention effect of ZL capsule on EndMT in HUVEC lines, and the experimental results showed that LDL could induce EndMT transformation in HUVECs, while ZL capsule could block the induction effect of LDL on HUVECs. According to the findings, ZL capsule has the potential to disrupt EC dysfunction, particularly due to its ability to inhibit EndMT.

The process of EndMT was initially observed in the development of heart valves, where it involves a transformation from epithelial to mesenchymal cells triggered by an external signal.<sup>30</sup> At the molecular scale, EndMT exhibits similarities to EMT in terms of its ability to facilitate tumor advancement, invasion, and metastasis. The frequently investigated molecular pathways implicated in EndMT encompass transforming growth factor  $\beta$  (TGF $\beta$ ), Notch, interleukin, and Hippo/YAP signaling.<sup>31</sup> YAP, a crucial intermediary of Hippo/YAP signaling and an essential controller of EndMT, has been confirmed to promote UO-induced kidney fibrosis via Hippo/YAP pathway<sup>32</sup> and improve renal fibrosis symptoms by inhibiting the occurrence of EndMT. In this study, we found that several components of ZL capsule had strong affinity with YAP protein, suggesting that YAP may be a potential therapeutic target for ZL capsule to inhibit EndMT in AS, which was further confirmed *in vivo* and *in vitro*, namely, ZL capsule significantly inhibited the activation of Hippo/YAP signal during AS. Taken together, these results provide strong evidence that ZL capsule could inhibit EndMT by regulating the Hippo/YAP signaling pathway and effectively prevent the progression of AS.

### Conflicts of interest

The authors declare that there are no conflicts of interest associated with the manuscript.

### Authors' contributions

Yanan Zhou: Writing original draft, Methodology, Investigation, Supervision. Hong Wang: Investigation, Preparation, Methodology, Data curation. Tao Bi: Methodology, Investigation. Pan Liang: Methodology, Investigation. Xinyue Liu: Methodology, Investigation. Hongping Shen: Methodology, Funding acquisition. Qin Sun: Methodology, Funding acquisition. Gang Luo: Methodology, Investigation. Ping Liu: Funding acquisition. Sijin Yang: Conceptualization, Funding acquisition, Supervision. Wei Ren: Conceptualization, Funding acquisition, Supervision, Writing—review & editing.

### Ethics statement

This study was carried out in accordance with the recommendations of regulations of the experimental animal ethics committee of Southwest Medical University. The protocol was approved by the experimental animal ethics committee of Southwest Medical University (No.20221202-001).

### Funding acknowledgments

This research was funded by Sichuan Administration of Traditional

Chinese Medicine (Number: 2023MS379, 2021DZ05), Sichuan Science and Technology Program (Number: 2022YFS0635, 2022YFS0618), Innovation Team and Talents Cultivation Program of National Administration of Traditional Chinese Medicine (Number: ZZYXCTD-C-202207), Innovation Team of Sichuan Provincial Administration of Traditional Chinese Medicine (Number: 2022C007).

### Declaration of competing interest

The authors declare that they have no known competing financial interests or personal relationships that could have appeared to influence the work reported in this paper.

### Data availability

The data used to support the findings of this study are included within the article. The supporting data is available upon reasonable request from the corresponding author.

### Acknowledgments

Thanks for the experiment conditions provided by Luzhou Key Laboratory for Prevention and Treatment of Cardiovascular and Cerebrovascular Diseases with Integrated Traditional Chinese and Western Medicine and the High-resolution Mass Spectrometry Testing Center of the Affiliated Traditional Chinese Medicine Hospital of Southwest Medical University.

### Abbreviations

ZL	Zhilong Huoxue Tongyu
TCM	traditional Chinese medicine
EndMT	Endothelial-mesenchymal transition
AS	atherosclerosis
HFD	high-fat diet
ATO	Atorvastatin calcium tablets
HUVECs	human umbilical vein endothelial cells
ox-LDL	oxidized low-density lipoprotein
WB	western blotting
CVD	Cardiovascular disease
EC	Endothelial cell
$\alpha$ -SMA	$\alpha$ -smooth muscle actin
FSP-1	fibroblast-specific protein 1
TC	total cholesterol
TG	total triglyceride
LDL-C	low-density lipoprotein cholesterol
HDL-C	high-density lipoprotein
H&E	Hematoxylin-Eosin
TGF $\beta$	transforming growth factor $\beta$

### References

- Amini M, Zayeri F, Salehi M. Trend analysis of cardiovascular disease mortality, incidence, and mortality-to-incidence ratio: results from global burden of disease study 2017. *BMC Publ Health*. 2021;21(1):401.
- Roth GA, Mensah GA, Johnson CO, et al. Global burden of cardiovascular diseases and Risk factors, 1990-2019: Update from the GBD 2019 study. *J Am Coll Cardiol*. 2020;76(25):2982–3021.
- Wolf D, Ley K. Immunity and inflammation in atherosclerosis. *Circ Res*. 2019;124(2):315–327.
- Kim JY, Choi BG, Jelinek J, et al. Promoter methylation changes in ALOX12 and AIRE1: novel epigenetic markers for atherosclerosis. *Clin Epigenet*. 2020;12(1):66.
- Libby P, Okamoto Y, Rocha VZ, Folco E. Inflammation in atherosclerosis: transition from theory to practice. *Circ J*. 2010;74(2):213–220.
- Pernow J, Jung C. The emerging role of arginase in endothelial dysfunction in diabetes. *Curr Vasc Pharmacol*. 2016;14(2):155–162.
- Claesson-Welsh L, Dejana E, McDonald DM. Permeability of the endothelial barrier: identifying and reconciling controversies. *Trends Mol Med*. 2021;27(4):314–331.
- Qu K, Wang C, Huang L, et al. TET1s deficiency exacerbates oscillatory shear flow-induced atherosclerosis. *Int J Biol Sci*. 2022;18(5):2163–2180.

9. Aniwan S, Pardi DS, Tremaine WJ, Loftus Ev Jr. Increased risk of acute myocardial infarction and heart failure in patients with inflammatory bowel diseases. *Clin Gastroenterol Hepatol*. 2018;16(10):1607–1615 e1601.
10. Epelman S, Liu PP, Mann DL. Role of innate and adaptive immune mechanisms in cardiac injury and repair. *Nat Rev Immunol*. 2015;15(2):117–129.
11. Li G, Shang C, Li Q, et al. Combined shikonin-loaded MPEG-PCL micelles inhibits effective transition of endothelial-to-mesenchymal cells. *Int J Nanomed*. 2022;17:4497–4508.
12. Miscianinov V, Martello A, Rose L, et al. MicroRNA-148b targets the TGF-beta pathway to regulate angiogenesis and endothelial-to-mesenchymal transition during skin wound healing. *Mol Ther*. 2018;26(8):1996–2007.
13. Evrard SM, Lecce L, Michelis KC, et al. Endothelial to mesenchymal transition is common in atherosclerotic lesions and is associated with plaque instability. *Nat Commun*. 2016;7, 11853.
14. Evrard SM, Lecce L, Michelis KC, et al. Corrigendum: endothelial to mesenchymal transition is common in atherosclerotic lesions and is associated with plaque instability. *Nat Commun*. 2017;8, 14710.
15. Moya IM, Halder G. Hippo-YAP/TAZ signalling in organ regeneration and regenerative medicine. *Nat Rev Mol Cell Biol*. 2019;20(4):211–226.
16. Yu Q, Li W, Jin R, et al. PI3Kgamma (phosphoinositide 3-kinase gamma) regulates vascular smooth muscle cell phenotypic modulation and neointimal formation through CREB (cyclic AMP-response element binding protein)/YAP (Yes-Associated protein) signaling. *Arterioscler Thromb Vasc Biol*. 2019;39(3):e91–e105.
17. Liang P, Mao L, Ma Y, Ren W, Yang S. A systematic review on Zhilong Huoxue Tongyu capsule in treating cardiovascular and cerebrovascular diseases: pharmacological actions, molecular mechanisms and clinical outcomes. *J Ethnopharmacol*. 2021;277, 114234.
18. Liu M, Pu Y, Gu J, et al. Evaluation of Zhilong Huoxue Tongyu capsule in the treatment of acute cerebral infarction: a systematic review and meta-analysis of randomized controlled trials. *Phytomedicine*. 2021;86, 153566.
19. Wang R, Liu M, Ren G, et al. Zhilong Huoxue Tongyu Capsules' Effects on ischemic stroke: an assessment using fecal 16S rRNA gene sequencing and untargeted serum metabolomics. *Front Pharmacol*. 2022;13, 1052110.
20. Mazhar M, Yang G, Xu H, et al. Zhilong Huoxue Tongyu capsule attenuates intracerebral hemorrhage induced redox imbalance by modulation of Nrf2 signaling pathway. *Front Pharmacol*. 2023;14, 1197433.
21. Liu M, Luo G, Liu T, et al. Zhilong Huoxue Tongyu capsule alleviated the pyroptosis of vascular endothelial cells induced by ox-LDL through miR-30b-5p/NLRP3. *Evid Based Complement Alternat Med*. 2022;2022, 3981350.
22. Solanki S, Dube PR, Tano JY, Birnbaumer L, Vazquez G. Reduced endoplasmic reticulum stress-induced apoptosis and impaired unfolded protein response in TRPC3-deficient M1 macrophages. *Am J Physiol Cell Physiol*. 2014;307(6):C521–C531.
23. Mazhar M, Yang G, Mao L, et al. Zhilong Huoxue Tongyu capsules ameliorate early brain inflammatory injury induced by intracerebral hemorrhage via inhibition of canonical NFsmall ka, cyrillicbeta signalling pathway. *Front Pharmacol*. 2022;13, 850060.
24. Saiki P, Yoshihara M, Kawano Y, Miyazaki H, Miyazaki K. Anti-inflammatory effects of heliangin from Jerusalem artichoke (*Helianthus tuberosus*) leaves might prevent atherosclerosis. *Biomolecules*. 2022;12(1).
25. Zhang F, Zhang R, Zhang X, et al. Comprehensive analysis of circRNA expression pattern and circRNA-miRNA-mRNA network in the pathogenesis of atherosclerosis in rabbits. *Aging (Albany NY)*. 2018;10(9):2266–2283.
26. Zhang Z, Chang LY, Lau AKH, et al. Satellite-based estimates of long-term exposure to fine particulate matter are associated with C-reactive protein in 30 034 Taiwanese adults. *Int J Epidemiol*. 2017;46(4):1126–1136.
27. Li X, Sun Z, Peng G, et al. Single-cell RNA sequencing reveals a pro-invasive cancer-associated fibroblast subgroup associated with poor clinical outcomes in patients with gastric cancer. *Theranostics*. 2022;12(2):620–638.
28. Wang C, Niimi M, Watanabe T, Wang Y, Liang J, Fan J. Treatment of atherosclerosis by traditional Chinese medicine: questions and quandaries. *Atherosclerosis*. 2018; 277:136–144.
29. Lovisa S, Fletcher-Sanankone E, Sugimoto H, et al. Endothelial-to-mesenchymal transition compromises vascular integrity to induce Myc-mediated metabolic reprogramming in kidney fibrosis. *Sci Signal*. 2020;13(635).
30. Laurent F, Girdziusaite A, Gamart J, et al. HAND2 target gene regulatory networks control atrioventricular canal and cardiac valve development. *Cell Rep*. 2017;19(8): 1602–1613.
31. Sabbineni H, Verma A, Artham S, et al. Pharmacological inhibition of beta-catenin prevents EndMT in vitro and vascular remodeling in vivo resulting from endothelial Akt1 suppression. *Biochem Pharmacol*. 2019;164:205–215.
32. Ren Y, Zhang Y, Wang L, et al. Selective targeting of vascular endothelial YAP activity blocks EndMT and ameliorates unilateral ureteral obstruction-induced kidney fibrosis. *ACS Pharmacol Transl Sci*. 2021;4(3):1066–1074.